arXiv:1408.0970v1 [hep-ex] 5 Aug 2014

August 6, 2014

Charm mixing and CP violation

Alberto C. dos Reis[1]

Centro Brasileiro de Pesquisas Físicas
Rio de Janeiro, Brazil

Experimental results on charm mixing and CP violation searches are reviewed. This paper focus on results released after FPCP 2013.

PRESENTED AT

Flavor Physics and CP Violation (FPCP-2014)
Marseille, France, May 26-30, 2014

[1]on behalf of the LHCb collaboration.

1 Introduction

In 2014 we celebrate the 40th anniversary of the discovery of the charm quark — the "November revolution". It took over 30 years of experimental efforts to achieve the necessary sensitivity for the establishment of charm mixing*, which happened in 2008 when of results from different experiments [1, 2, 3, 4] were combined.

This year we also celebrate the 50th anniversary of the discovery of *CP* violation. While the *CP* violation is well established in decays of neutral kaons and B mesons, in charm it has not been observed yet.

Mixing and *CP* violation in charm are regarded as promising fields in the search for new physics, especially after the commissioning of the LHC. The interpretation of the experimental results, however, is still problematic. Predictions of the Standard Model (SM) contribution to the mixing rate and *CP* asymmetries suffer from uncertainties on the hadronic matrix elements.

In this paper we review the main experimental results on charm mixing and *CP* violation searches that were released after the 2013 edition of FPCP, in Búzios.

2 Time-dependent measurements

2.1 Mixing and CP violation search with WS $D^0 \to K\pi$

The measurement of the time-dependent ratio of the "wrong-sign" $D^0 \to K^+\pi^-$ (WS) to the "right-sign" (RS) $D^0 \to K^-\pi^+$ decay rates is the most sensitive method for observing D^0–$\overline{D}^0$ oscillations. The RS decay rate is, for any practical purpose, given by the Cabibbo favoured (CF) transition $D^0 \to K^-\pi^+$, as illustrated in Fig. 1. There is a negligibly small contribution from processes where a net oscillation to a $\overline{D}^0$ is followed by the doubly Cabibbo suppressed (DCS) transition $\overline{D}^0 \to K^-\pi^+$. For the WS decay rate, on the other hand, there are two competing contributions: the direct DCS transition $D^0 \to K^+\pi^-$; a net oscillation to a $\overline{D}^0$ followed by the CF transition $\overline{D}^0 \to K^+\pi^-$. The concurrence of these two paths allows one to extract the mixing parameters.

An extra bonus of this method comes from the fact that the WS and RS decays are expected to have the same decay-time acceptance, so the ratio between WS and RS events cancels most of the systematic uncertainties affecting the determination of the yields as a function of the decay time.

*In the literature the terms "mixing" and "oscillations" are used interchangeably. Mixing arises from the fact that mass and flavour eigenstates are not identical. One manifestation of mixing is the existence of mass eigenstates with different lifetimes. Mixing also induces flavour oscillations, in-flight transitions between a neutral meson and its antiparticle. Oscillations are characterized by a sinusoidal behavior of the time evolution of neutral system. In this review the notation "charm mixing" is used as a generic designation of both mixing and oscillations.

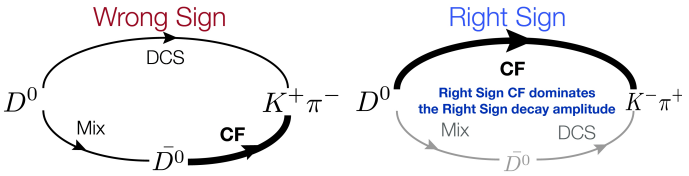

Figure 1: The two paths for WS $D^0 \to K^+\pi^-$ decays. The RS $D^0 \to K^-\pi^+$ decay is completely dominated by the CF transition.

The mixing rate is characterized by two dimensionless parameters x and y,

$$x \equiv \frac{m_1 - m_2}{\Gamma_D} = \frac{\Delta m}{\Gamma_D}, \qquad y \equiv \frac{\Gamma_1 - \Gamma_2}{2\Gamma_D} = \frac{\Delta\Gamma}{2\Gamma_D}, \tag{1}$$

where $m_{1,2}$ and $\Gamma_{1,2}$ are the masses and widths of the mass eigenstates, and $\Gamma_D \equiv (\Gamma_1 + \Gamma_2)/2$ is the inverse of the average D^0 lifetime.

In the $D^0 \to K\pi$ method one has to account for the relative strong phase between the amplitudes for the CF and DCS decays,

$$\frac{A_{K^+\pi^-}}{\overline{A}_{K^+\pi^-}} = -\sqrt{R_D}\, e^{-i\delta_{K\pi}},$$

The mixing parameters extracted with this method are rotated with respect to those defined by eq. 1,

$$x' = x\cos\delta_{K\pi} + y\sin\delta_{K\pi}, \qquad y' = y\cos\delta_{K\pi} - x\sin\delta_{K\pi}.$$

The relative phase $\delta_{K\pi}$ is an external input that is measured in e^+e^- storage rings [6, 7] where, at a center of mass energy corresponding to the $\psi(3770)$ resonance, a $D\overline{D}$ pair is produced in a quantum correlated state with $C = 1$.

In the limit of small mixing ($x, y \ll 1$) and neglecting CP violation, the time-dependent ratio of WS to RS decay rates is given by,

$$R(t) \approx R_D + \sqrt{R_D}y'\frac{t}{\tau} + \frac{x'^2 + y'^2}{4}\left(\frac{t}{\tau}\right)^2, \tag{2}$$

where t/τ is the decay time expressed in units of the average D^0 lifetime τ. The decay time t is computed in the D^0 rest frame using the measured D^0 mass, the distance from the production to the decay positions and the D^0 momentum, $t = m_D\Delta\vec{X}\cdot\vec{p}/|\vec{p}|^2$. The typical decay time resolution in LHCb is approximately 0.1τ.

The first term in the right side of Eq. (2) is the time-integrated ratio between the DCS and CF decay rates. The linear term in t/τ corresponds to the interference between WS decays with and without oscillations, whereas the quadratic term accounts for the pure mixing contribution.

If CP violation is not neglected, the time-dependent ratio between WS and RS decays may differ for D^0 and $\overline{D}^0$. The WS-to-RS ratios for initially produced D^0 and $\overline{D}^0$, denoted by $R^+(t)$ and $R^-(t)$, respectively, are functions of six independent mixing parameters $(R_D^{\pm}, x'^{2\pm}, y'^{\pm})$. Different values for (x'^{2+}, y'^{+}) and (x'^{2-}, y'^{-}) imply CP violation, either in mixing ($|q/p| \neq 1$) or in the interference between the amplitudes for decays with and without a net oscillation ($\phi \equiv \arg[qA(\overline{D}^0 \to K^-\pi^+)/pA(D^0 \to K^-\pi^+)] - \delta_{K\pi} \neq 0$).

Using the full data set from the 2011 and 2012 runs, LHCb reported on an improved measurement of the CP-averaged charm mixing parameters and a search for CP violation using the $D^0 \to K^+\pi^-$ decay[5]. The measurement is based on approximately 2.3×10^5 WS and 5.3×10^7 RS decays. The $D^0\pi^+$ invariant mass spectrum is shown in Fig. 2. The background under the WS signal is dominated by favored $\overline{D}^0 \to K^+\pi^-$ decays associated to a random slow pion.

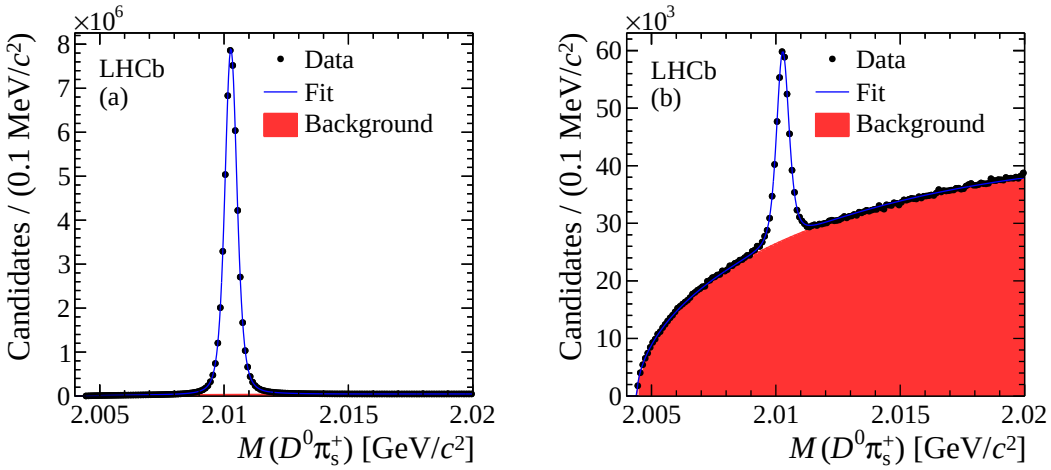

Figure 2: The RS $D^0 \to K^-\pi^+$ (left) and WS $\overline{D}^0 \to K^+\pi^-$ (right) time-integrated $D^0\pi^+$ mass distributions from LHCb (3 fb^{-1}). The projection of the fits (blue line) are overlaid. In the bottom plots the normalized residuals between the data points and fits are shown.

The data shown in Fig. 2 is divided into thirteen bins of decay time with approximately the same number of decays. The RS and WS yields are determined from thirteen independent fits of the $M(D^0\pi^+)$ distribution, where only D^0 candidates with mass within ± 24 MeV/c^2 of the nominal value are considered. The mixing parameters are determined by minimizing a χ^2 variable that includes the observed and predicted ratios, and terms accounting for the systematic effects associated to candidates from b-hadron decays, double misidentification of the final state particles and instrumental asymmetries in the $K^-\pi^+/K^+\pi^-$ reconstruction efficiency.

Fits are performed under different hypothesis: allowing for direct and indirect CP

violation; allowing only for indirect CP violation, which constrains $R_D^{\pm}$ to a single value; a CP-conserving fit, constraining all mixing parameters to be common to D^0 and $\overline{D}^0$.

The fit results are shown in Fig. 3. The efficiency-corrected ratios $R^+(t)$ and $R^-(t)$ and the difference $R^+(t) - R^-(t)$ are displayed (black full circles with error bars) as functions of the decay time, in units of D^0 lifetime, with the projections of the fit results (lines in blue) superimposed. The slope of the $R^+(t) - R^-(t)$ difference is approximately 5% of the individual slopes of the $R^+(t)$ and $R^-(t)$ distributions and is consistent with zero.

The signal for direct CP violation would be a nonzero intercept at $t = 0$ of the $R^+(t) - R^-(t)$ distribution. This intercept is parameterized by asymmetry A_D,

$$A_D \equiv \frac{R_D^+ - R_D^-}{R_D^+ + R_D^-}.$$

The asymmetry A_D is measured from the fit with all forms of CP violation allowed. The result is $A_D = (-0.7 \pm 1.9)\%$.

The fit results are summarized in Table 1 with statistical and systematic uncertainties, respectively.

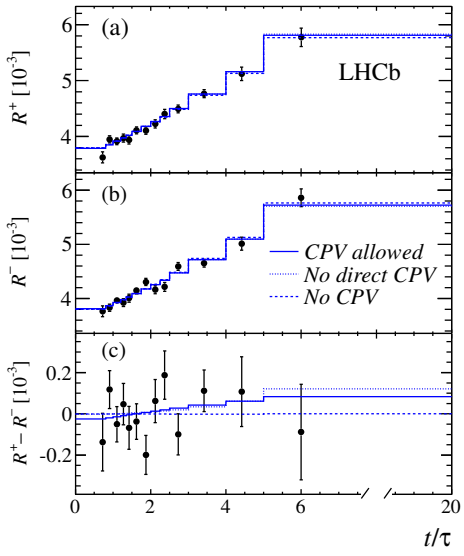

Figure 3: Efficiency-corrected ratios of WS-to-RS yields, R^+ and R^-, for D^0 and $\overline{D}^0$, and their difference as a function of the decay time in units of D^0 lifetimes, from LHCb. Projections of the three types of fits are superimposed.

The central values and confidence regions in the (x'^2, y') plane are shown in Fig. 4 for the three fits. The data is compatible with CP conservation.

Table 1: Measured parameters of $D^0-\overline{D}^0$ mixing, obtained from the ratio of wrong sign to right sign $D^0 \to K^+\pi^-$ decays, for different hypothesis on *CP* symmetry.

Parameter	Fit result
Direct and indirect *CP* violation	
$R_D^+(\times 10^{-3})$	$3.545 \pm 0.082 \pm 0.048$
$y'^+(\times 10^{-3})$	$5.1 \pm 1.2 \pm 0.7$
$x'2+(\times 10^{-5})$	$4.9 \pm 6.0 \pm 3.6$
$R_D^-(\times 10^{-3})$	$3.591 \pm 0.081 \pm 0.048$
$y'^-(\times 10^{-3})$	$4.5 \pm 1.2 \pm 0.7$
$x'2-(\times 10^{-5})$	$6.0 \pm 5.8 \pm 3.6$
χ^2/ndof	85.9/98
Indirect *CP* violation	
$R_D(\times 10^{-3})$	$3.568 \pm 0.0058 \pm 0.033$
$y'^+(\times 10^{-3})$	$4.8 \pm 0.9 \pm 0.6$
$x'2+(\times 10^{-5})$	$6.4 \pm 4.7 \pm 3.0$
$y'^-(\times 10^{-3})$	$4.8 \pm 0.9 \pm 0.6$
$x'2-(\times 10^{-5})$	$4.6 \pm 4.6 \pm 3.0$
χ^2/ndof	86.0/99
No *CP* violation	
$R_D(\times 10^{-3})$	$3.568 \pm 0.0058 \pm 0.033$
$y'(\times 10^{-3})$	$4.8 \pm 0.8 \pm 0.5$
$x'2(\times 10^{-5})$	$5.5 \pm 4.2 \pm 2.6$
χ^2/ndof	86.4/101

2.2 A_Γ from $D^0 \to K^+K^-$ and $D^0 \to \pi^+\pi^-$

Decays of D^0 to final states that are *CP* eigenstates, such as $D^0 \to K^-K^+$ and $D^0 \to \pi^-\pi^+$, provide an alternative way to search for *CP* violation in mixing. Under the assumption of no direct *CP* violation, the decay time distributions, to a good approximation, can be described by pure exponentials with effective widths[8],

$$\begin{aligned}
\hat{\Gamma}(D^0 \to h^+h^-) &= \Gamma_D \left[1 + \left|\frac{q}{p}\right| (y\cos\phi - x\sin\phi)\right], \\
\hat{\Gamma}(\overline{D}^0 \to h^+h^-) &= \Gamma_D \left[1 + \left|\frac{p}{q}\right| (y\cos\phi + x\sin\phi)\right], \\
\hat{\Gamma}(D^0 \to K^-\pi^+) &= \hat{\Gamma}(\overline{D}^0 \to K^+\pi^-) = \Gamma_D, \qquad (3)
\end{aligned}$$

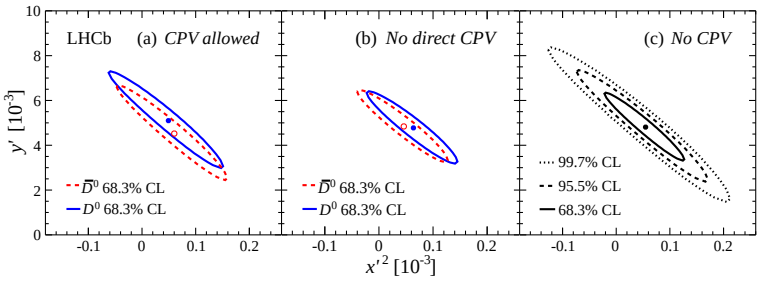

Figure 4: Two-dimensional CL contours in the (x'^2, y') plane, from LHCb, for the three types of fit: (a) no restriction on *CP* violation; (b) assuming no direct *CP* violation; (c) assuming *CP* conservation.

where Γ_D is the average D^0 lifetime, ϕ is the relative phase between the amplitudes for decays with and without mixing, and $h = K, \pi$.

Two observables can be built from the effective lifetimes:

$$y_{CP} = \frac{\hat{\Gamma}_{D^0 \to h^+h^-} + \hat{\Gamma}_{\overline{D}^0 \to h^+h^-}}{2\Gamma_D} - 1,$$

and

$$A_\Gamma \equiv \frac{\hat{\Gamma}(D^0 \to h^+h^-) - \hat{\Gamma}(\overline{D}^0 \to h^+h^-)}{\hat{\Gamma}(D^0 \to h^-h^+) + \hat{\Gamma}(\overline{D}^0 \to h^+h^-)} \simeq \left(\frac{1}{2}A_m y \cos\phi - x \sin\phi\right),$$

with

$$A_m = \frac{|q/p|^2 - |p/q|^{-2}}{|q/p|^2 + |p/q|^{-2}}.$$

Any difference between $\hat{\Gamma}_{D^0 \to h^+h^-}$ and $\hat{\Gamma}_{D^0 \to K\pi}$ is a signal of mixing, whereas any difference between $\hat{\Gamma}_{D^0 \to h^+h^-}$ and $\hat{\Gamma}_{\overline{D}^0 \to h^+h^-}$ means indirect *CP* violation, either through the phase ϕ or through A_m.

A measurement of A_Γ using the decays $D^0 \to K^-K^+$ and $D^0 \to \pi^-\pi^+$ was performed by LHCb, with 1 fb^{-1} of pp collisions at 7 TeV[9]. In this analysis flavor tagging is performed through the charge of the slow pion in the chain $D^{*+} \to D^0\pi^+$, $D^0 \to hh$. The reconstructed momentum of the slow pion is constrained to the pp interaction vertex, a technique that improves the signal resolution in the mass difference $\Delta m = m(hh\pi) - m(hh)$ spectrum, with a consequent improvement in the signal-to-noise ratio.

The selected sample contains 3.11×10^6 $D^0 \to K^+K^-$ and 1.03×10^6 $D^0 \to \pi^+\pi^-$ candidates. For each final state the selected sample is divided into eight subsets, according to the flavor of the D^0, the magnet polarity and data taking period. The latter accounts for important changes in the trigger configuration during the 2011 run. In the left plot of Fig. 5 the Δm distribution of one of the eight subsets is shown, for the $D^0 \to K^-K^+$ channel.

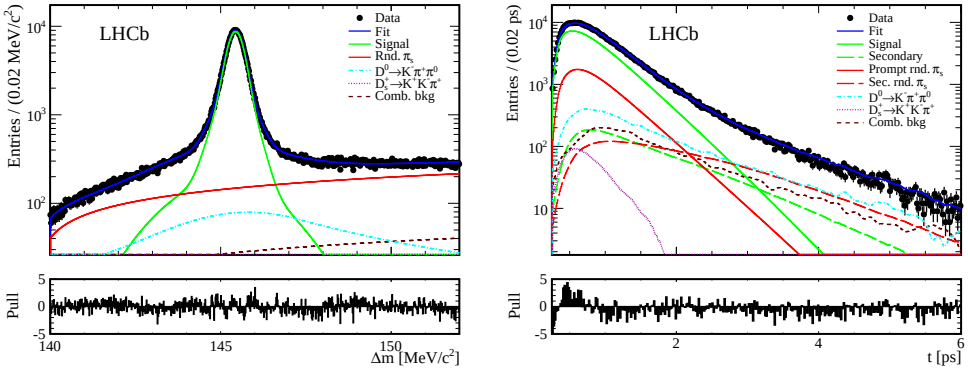

Figure 5: Left: mass difference $m(K^-K^+\pi^-) - m(K^+K^-)$, from LHCb, with the fit result superimposed including the various background components. Right: the decay time distribution of $\overline{D}^0 \to K^-K^+$ candidates with fit results superimposed. Both plots correspond to one of the eight subsets (see text for more retails).

The determination of the effective lifetimes is performed in two stages. In the first stage, a bi-dimensional fit to the $m(hh)$ and Δm distributions is carried out, fixing the fractions of the signals and the main classes of background, namely true D^0 associated to a random slow pion, partially reconstructed decays and combinatorial background.

D^0 candidates from decays of b-hadrons, or secondary D^0, is an important background that cannot be separated by the mass fit. Since b-hadron have long lifetimes, this background is more important at larger values of the decay time. The impact parameter with respect to the primary pp interaction vertex is used to discriminate the promptly produced D^0 candidates from secondary D^0. In Fig. **??** the distribution of an impact parameter variable is shown for three decay time intervals.

The effective lifetimes are extracted in the second stage by a two-dimensional fit to the impact parameter and decay time distributions. The fit result, for one of the eight subsets of the $D^0 \to K^-K^+$ sample, is displayed in the right plot of Fig. **??**.

An alternative method is used as a check to the nominal unbinned fit results. The data is divided in bins of decay time with approximately equal population. The ratio of $\overline{D}^0$ to D^0, is computed in each bin and the value of A_Γ is obtained from a linear χ^2 minimization. The results obtained with the unbinned and binned methods are in good agreement.

The results obtained by LHCb with 1.0 fb^{-1} are:

$$A_\Gamma(KK) = \quad (-0.035 \pm 0.062 \pm 0.012)\% \tag{4}$$

$$A_\Gamma(\pi\pi) = \quad (0.033 \pm 0.106 \pm 0.014)\% \tag{5}$$

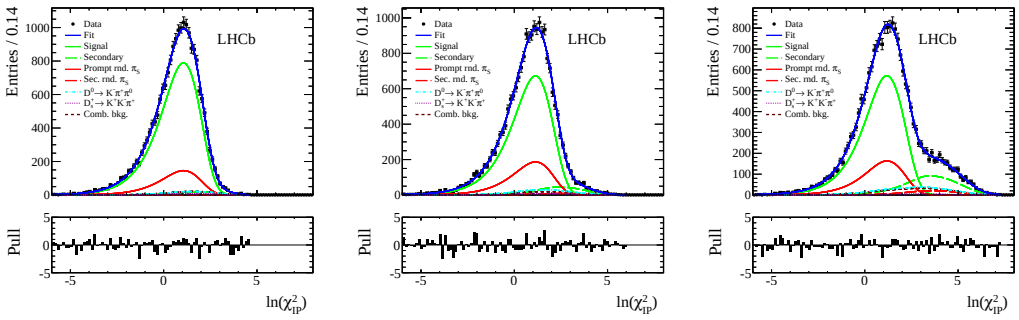

Figure 6: The distribution of the logarithm of an impact parameter variable for three D^0 decay time intervals. For longer decay times the contribution from D^0 produced in B decays becomes more important.

The measured values of $A_\Gamma(KK)$ and $A_\Gamma(\pi\pi)$ are consistent with each other and with the no CP violationhypothesis.

2.3 Mixing from time-dependent $D^0 \to K^0_S\pi^+\pi^-$ Dalitz plot analysis

A direct measurement of the mixing parameters x and y is accomplished by a time-dependent amplitude analysis of the self-conjugate decay $D^0 \to K^0_S\pi^+\pi^-$. The D^0 meson is produced in a well defined flavour state. Since the final state is reachable by both D^0 and $\overline{D}^0$, at any later time one has a mixture of both flavour eigenstates. The dominant contribution to the D^0 Dalitz plot is the "RS" CF intermediate state $K^{*-}\pi^+$ ($K^{*+}\pi^-$, for the $\overline{D}^0$). There is also a small "WS" $K^{*+}\pi^-$ component, either from a direct DCS transition or from a net $D^0 \to \overline{D}^0$ oscillation followed by the CF $\overline{D}^0 \to K^{*+}\pi^-$. The RS and WS components become time dependent, and this is the mixing signature. Assuming no direct CP violation, the mixing parameters x and y are determined by a simultaneous fit of the D^0 and $\overline{D}^0$ Dalitz plots as a function of the decay proper time.

A time-dependent Dalitz plot analysis of the $D^0 \to K^0_S\pi^+\pi^-$ decay was published by Belle[10], based on 1.23×10^6 signal events with a purity of 95.6%. The Dalitz plot (DP) distribution is described in terms of the two invariants $s_\pm \equiv m^2(K^0_S\pi^\pm)$. The decay amplitudes are parameterized as a sum of quasi-two-body amplitudes,

$$A(s_+, s_-) = \sum a_k e^{i\delta_k} A_k(s_+, s_-), \tag{6}$$

for a sample containing only D^0 decays, and

$$\overline{A}(s_+, s_-) = \sum \overline{a}_k e^{i\overline{\delta}_k} A_k(s_-, s_+), \tag{7}$$

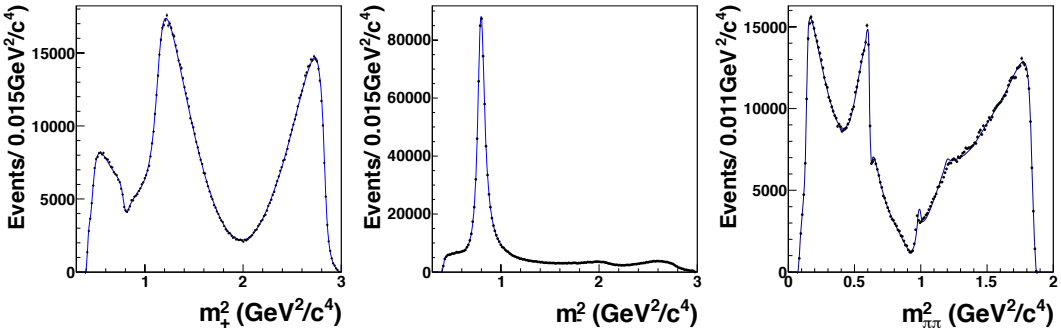

Figure 7: Dalitz plot projections onto the m_+, m_- and $m_{\pi\pi}$ axes, from Belle's $D^0 \to K^0_S\pi^-\pi^+$ candidates.

for the sample containing only $\overline{D}^0$ decays. The assumption of no direct *CP* violationimply the equality of the complex coefficients $\overline{a}_k e^{i\overline{\delta}_k} = a_k e^{i\delta_k}$. The decay model has The dependence on x and y appears when the expressions for the decay matrix elements are squared.

A Dalitz plot fit is performed assuming no *CP* violation, having as free parameters x, y, the D^0 lifetime, the parameters defining the proper time resolution function, and the parameters of the decay amplitude model. A fit allowing for *CP* violation is also performed and includes two more free parameters, $|q/p|$ and $\phi = \arg(q/p)$.

The two-body mass projections of the $D^0 \to K^0_S\pi^-\pi^+$ candidates from Belle are shown in Fig. 7. The decay model has 14 resonances, a K-matrix for $\pi\pi$ S-wave, effective range (LASS) for $K^0_S\pi$ S-wave (40 free parameters), but only an approximate solution found. The uncertainty in the decay amplitude model is the dominant systematic effect. The measured values of x and y are shown in Table 2.

The two-dimensional confidence level contours are shown in Fig. 8. The significance of D^0–$\overline{D}^0$ mixing is estimated to be 2.5 standard deviations from the no-mixing point ($x=y=0$). In spite of statistical significance bellow three standard deviations, this is the most precise measurement of the mixing parameters x and y. No evidence for *CP* violation was found.

Table 2: Measured parameters of $D^0-\overline{D}^0$ mixing (%) from Belle's time dependent $D^0 \to K^0_S h^+h^-$ Dalitz plot analyses, for different hypotheses on CP symmetry.

Parameter	Fit result
no CPV	
$x(\%)$	$0.56 \pm 0.19\ ^{+0.07}_{-0.13}$
$y(\%)$	$0.30 \pm 0.15\ ^{+0.05}_{-0.08}$
CPV allowed	
$x(\%)$	$0.56 \pm 0.19^{+0.07}_{-0.11}$
$y(\%)$	$0.30 \pm 0.15^{+0.05}_{-0.09}$
$\lvert q/p\rvert$	$0.90^{+0.16\ +0.08}_{-0.15\ -0.07}$
$\arg(q/p)(^\circ)$	$-6 \pm 11 \pm 3\ ^{+3}_{-4}$

3 CP violation searches in time-integrated rates

3.1 ΔA_{CP} from $\overline{B} \to D^0\mu^- X$

The time-integrated CP asymmetry in D^0 decays to a CP eigenstate f ($f = K\overline{K}, \pi\pi$) is mostly a measurement of direct CP violation,

$$A_{CP}(f) \equiv \frac{\Gamma(D^0 \to f) - \Gamma(\overline{D}^0 \to f)}{\Gamma(D^0 \to f) + \Gamma(\overline{D}^0 \to f)} \ \simeq\ a^{\rm dir}_{CP}(f) + \frac{\langle t \rangle}{\tau} a^{\rm ind}_{CP},$$

The term $a^{\rm ind}_{CP}$ represents CP violation in mixing and/or in interference between mixing and decay. It is universal, to a good approximation, with a contribution that depends on the experimental decay-time acceptance.

In the SM, direct CP asymmetry in K^-K^+ and $\pi^-\pi^+$ final states are expected to have opposite signs, so measuring their difference $\Delta A_{CP} \equiv A_{CP}(K^-K^+) - A_{CP}(\pi^-\pi^+)$, one benefits not only from from a higher sensitivity to CP violation and from the cancellation of systematics and production and detection asymmetries.

LHCb released a new ΔA_{CP} measurement[12] using D^0 decays from partially reconstructed $\overline{B} \to D^0\mu^- X$ decays. The full run I data set (3 fb^{-1}) contains 1.99×10^6 and 0.78×10^6 K^-K^+ and $\pi^-\pi^+$ candidates. The LHCb signals are shown in Fig. 9. These events, with the D^0 flavour tagged by the muon sign, form an independent set from that containing D^0 directly produced in the primary pp interaction and tagged by the pion sign in $D^{*+} \to D^0\pi^+$.

LHCb measures the total, or *raw* charge asymmetry,

$$A_{\rm raw} = \frac{\Gamma(D^0 \to f)\varepsilon(\mu^-)\mathcal{P}(D^0) - \Gamma(\overline{D}^0 \to f)\varepsilon(\mu^+)\mathcal{P}(\overline{D}^0)}{\Gamma(D^0 \to f)\varepsilon(\mu^-)\mathcal{P}(D^0) + \Gamma(\overline{D}^0 \to f)\varepsilon(\mu^+)\mathcal{P}(\overline{D}^0)} \ \simeq\ A^f_{CP} + A^\mu_D + A^B_{\mathcal{P}}.$$

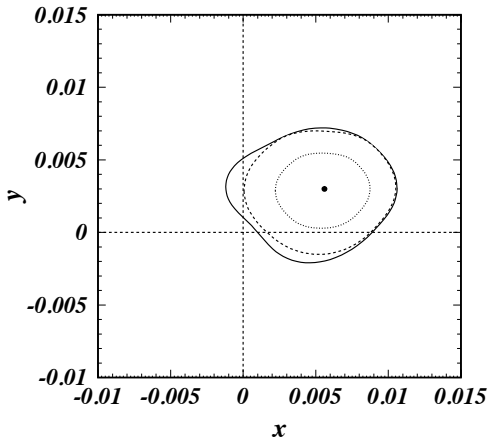

Figure 8: Confidence level contours in the x, y plane from Belle fit to the $D^0 \to K^0_S\pi^+\pi^-$ Dalitz plot. The dotted and dashed lines indicate the 68.3% and 95% CL contours from the *CP* -conserving fit. The solid line represents the 95% CL contour for the *CP* violation-allowed fit.

The detection and production asymmetries are, to first order, independent of the D^0 decay and cancel in the difference between the K^-K^+ and $\pi^-\pi^+$ raw asymmetries,

$$\Delta A_{CP} = A_{\rm raw}(K^-K^+) - A_{\rm raw}(\pi^-\pi^+) \simeq A_{CP}(K^-K^+) - A_{CP}(\pi^-\pi^+)$$

Second order effects are studied and accounted by as a systematic uncertainty. Using the Cabibbo favoured decays $D^0 \to K^-\pi^+$, $D^+ \to K^-\pi^+\pi^+$ and $D^+ \to K^0_S\pi^+$, the asymmetries A^μ_D and $A^B_{\mathcal{P}}$ are determined, allowing the measurement of the individual asymmetries:

$$A_{\rm raw}(K^-\pi^+) = A^\mu_D - A^B_{\mathcal{P}} - A_D(K^-\pi^+),$$

$$A_{CP}(K^-K^+) = A_{\rm raw}(K^-K^+) - A_{\rm raw}(K^-\pi^+) - A_D(K^-\pi^+)$$

The results from the updated LHCb measurement are

$$\begin{aligned} \Delta A_{CP} = &\quad (0.14 \pm 0.16 \pm 0.08)\%, \\ A_{CP}(KK) = &\quad (-0.06 \pm 0.15 \pm 0.010)\%, \\ A_{CP}(\pi\pi) = &\quad (-0.20 \pm 0.15 \pm 0.10)\%, \end{aligned} \tag{8}$$

No evidence for *CP* violation is found in this measurement. A world average of ΔA_{CP} and of the individual asymmetries was computed by the authors of Ref. [12]. An overview of the various measurements of ΔA_{CP} is shown in the plot on the left in

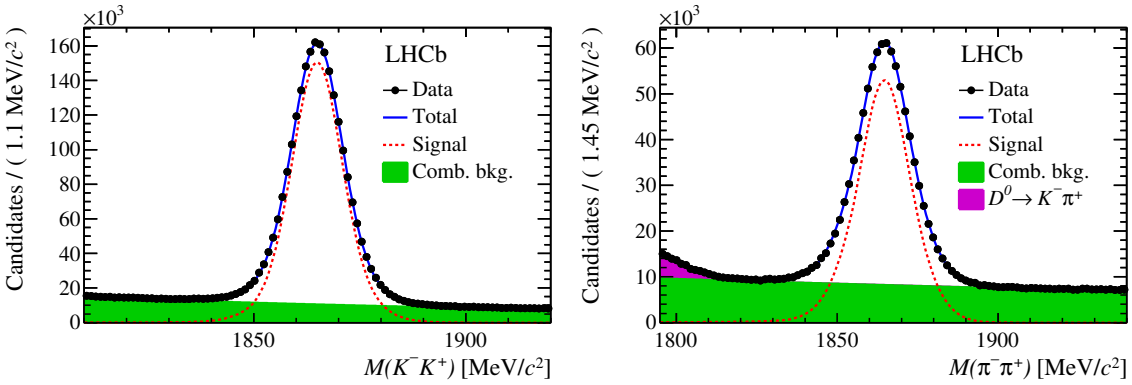

Figure 9: Invariant mass distributions of muon-tagged $D^0 \to K^-K^+$ (left) and $D^0 \to \pi^-\pi^+$ (right), from LHCb, with fit results superimposed.

Fig. 10. A world average, $\Delta A_{CP} = (-0.25 \pm 0.11)\%$ is obtained neglecting indirect CP violation effects. In the right plot of Fig. 10 an overview of the existing $A_{CP}(KK)$ and $A_{CP}(\pi\pi)$ are shown. World averages are found to be $A_{CP}(KK) = (-0.15 \pm 0.11)\%$ and $A_{CP}(\pi\pi) = (0.10 \pm 0.12)\%$ with a correlation $\rho = 0.57$.

3.2 $D^+_{(s)} \to K^0_S h^+$

Direct CP violation searches in charged D mesons are a natural complement to the measurements performed with neutral D. In particular, the modes $D^+ \to K^0_S K^+$ and $D^+_s \to K^0_S \pi^+$ have very similar amplitudes as those for $D^0 \to K^+K^-$ and $D^0 \to \pi^+\pi^-$.

LHCb measures the CP asymmetry in $D^+ \to K^0_S K^+$ and $D^+_s \to K^0_S \pi^+$ using the full 3 fb^{-1} data set from run I (2011+2012)[16]. The signal yields are 1.0×10^6 $D^+ \to K^0_S K^+$ and 1.2×10^5 $D^+_s \to K^0_S \pi^+$ decays. The analysis uses only K^0_S that decay at the vertex detector. Since these are very short lived K^0_S, the contribution to the measured charge asymmetry from CP violation in $K^0 - \overline{K}^0$ mixing is found to be negligible. In Fig. 11, the invariant mass distributions of the selected candidates are shown.

The observed charge asymmetry is a sum of the physical CP asymmetry plus contributions from production and detection asymmetries,

$$\mathcal{A}_{\rm raw}^{D^+_{(s)} \to K^0_S h^+} \approx \mathcal{A}_{CP}^{D^+_{(s)} \to K^0_S h^+} + \mathcal{A}_{\rm prod}^{D^+_{(s)}} + \mathcal{A}_{\rm det}^{h^+} + \mathcal{A}_{K^0},$$

The two observables, $\mathcal{A}_{CP}^{D^+ \to K^0_S K^+}$ and $\mathcal{A}_{CP}^{D^+_s \to K^0_S \pi^+}$ are obtained from five measurements, namely the charge asymmetries of the four Cabibbo favoured decays $D^+_{(s)} \to K^0_S h^+$ $(h = K, \pi)$ plus the asymmetry of $D^+_s \to \phi\pi^+$, used as a control

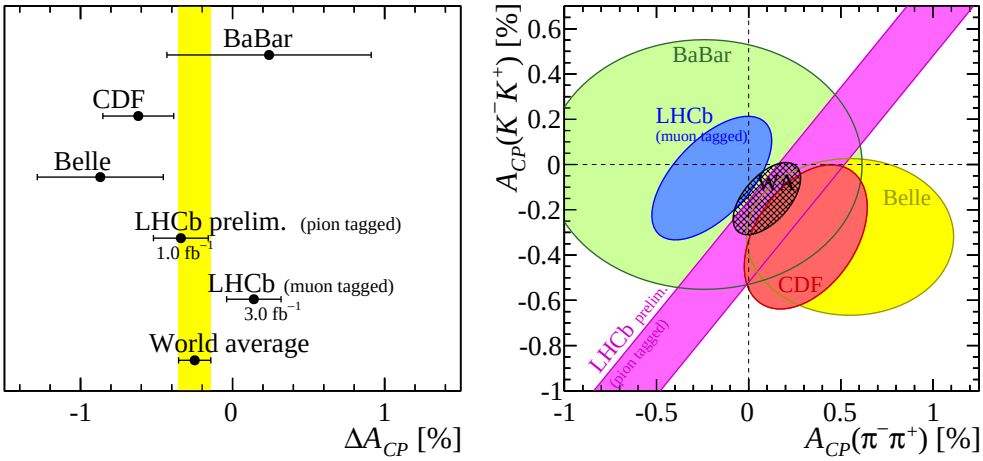

Figure 10: Overview of *CP* violation measurements in $D^0 \to K^-K^+$ and $D^0 \to \pi^-\pi^+$ decays from [11], [12], [13], [14], and [15]. On the left, measurements of the difference, ΔA_{CP} are shown together with the world average. On the right, the $A_{CP}(KK)$ versus $A_{CP}(\pi\pi)$ plane with the 68% confidence level contours is displayed. The new world averages are obtained neglecting any effect from indirect *CP* violation. Reproduced from the supplementary material of Ref. [12].

channel:

$$\begin{aligned}
\mathcal{A}_{CP}^{D^+\to K_S^0K^+} &\approx \left[\mathcal{A}_{\rm meas}^{D^+\to K_S^0K^+} - \mathcal{A}_{\rm meas}^{D_s^+\to K_S^0K^+}\right] - \left[\mathcal{A}_{\rm meas}^{D^+\to K_S^0\pi^+} - \mathcal{A}_{\rm meas}^{D_s^+\to \phi\pi^+}\right] - \mathcal{A}_{K^0}, \\
\mathcal{A}_{CP}^{D_s^+\to K_S^0\pi^+} &\approx \mathcal{A}_{\rm meas}^{D_s^+\to K_S^0\pi^+} - \mathcal{A}_{\rm meas}^{D_s^+\to \phi\pi^+} - \mathcal{A}_{K^0}.
\end{aligned}$$

Only K_S^0 with short decay time are used, the contribution from *CP* violation and K^0–$\overline{K}^0$ mixing is negligible. The value for $\mathcal{A}_{K^0}$ is $(0.7\pm0.2)\%$, and is dominated by the difference between K^0 and $\overline{K}^0$ in interaction with the detector material, $\sigma(K^0N) \neq \sigma(\overline{K}^0N)$.

The cancellation of the production and detection asymmetries is ensured by a event weighting procedure, used to equalize small differences in kinematic distributions of the final states. In addition, fiducial cuts remove a small fraction of events with large raw asymmetries in the momentum space. In these events the lowest momentum particle tends to be deflected out of the detector.

The values of $A_{CP}(D^+ \to K_S^0K^+)$ and $A_{CP}(D_s^+ \to K_S^0\pi^+)$ are consistent with zero:

$$\begin{aligned}
A_{CP}^{D^+\to K_S^0K^+} &= (+0.03 \pm 0.17 \pm 0.14)\% \\
A_{CP}^{D_s^+\to K_S^0\pi^+} &= (+0.38 \pm 0.46 \pm 0.17)\%.
\end{aligned}$$

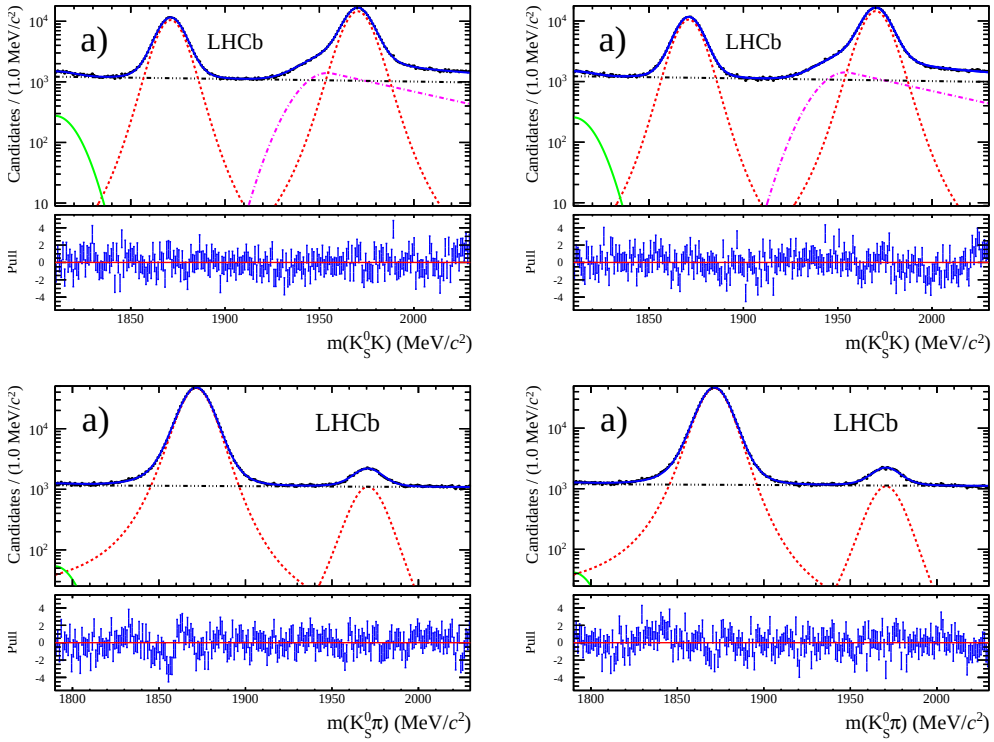

Figure 11: Invariant mass distributions for the $D^+_{(s)} \to K^0_S K^+$ (top left), $D^-_{(s)} \to K^0_S K^-$ (top right), $D^+_{(s)} \to K^0_S \pi^+$ (bottom left) and$D^-_{(s)} \to K^0_S \pi^-$ (bottom right), from LHCb. The fit result is overlaid, showing the contribution from the different backgrounds.

(9)

3.3 $D^+ \to \pi^-\pi^+\pi^+$

Three-body decays offer unique opportunities in *CP* violation searches:

- asymmetries localized in specific regions of the Dalitz may be significantly larger than phase-space integrated ones, e.g. large asymmetries observed in charmless $B^+ \to h_1^- h_2^+ h_3^+$ (see I. Bediaga's talk in this conference);
- local *CP* asymmetries may change sign across the phase space;
- the pattern of local *CP* asymmetries brings additional information on the underlying dynamics (other than a single number).

The main strategy in the search for *CP* violation in three-body decays of D mesons is to perform a direct, model-independent comparison between $D^+_{(s)}$ and $D^-_{(s)}$ Dalitz plots. The comparison can be made either using a binned [17] or an unbinned [18] approach. The drawback to this approach is that, in the absence of a signal, one cannot set limits on *CP* violation effects. In the event of a *CP* violation signal, this procedure should be followed by a full amplitude analysis.

The binned technique is being largely utilized to search for localized *CP* asymmetries. The combined $D^\pm_{(s)}$ Dalitz plot is divided into bins. For each the statistical significance of the asymmetry

$$S^i_{CP} = \frac{N_i(D^+) - \alpha N_i(D^-)}{\sqrt{\alpha[\sigma_i^2(D^+) + \sigma_i^2(D^-)]}} \tag{10}$$

is calculated, where $N_i(D^+)$ and $N_i(D^-)$ are the number of D^+ and D^- decays in each bin i. The uncertainties $\sigma_i(D^+)$ and $\sigma_i(D^-)$ are usually taken as $\sqrt{N_i(D^+)}$ and $\sqrt{N_i(D^-)}$. The parameter α is the ratio between the total number of D^+ and D^- events and is used as a correction due to a global production asymmetry.

The distribution of S^i_{CP} is normal under the hypothesis of *CP* conservation. A χ^2 test using $\chi^2 = \sum_{i=1}^{N} S^i_{CP}$ provides a numerical evaluation for the degree of confidence for the assumption that the differences between the D^+ and D^- Dalitz plots are driven only by statistical fluctuations.

LHCb used this model independent approach to look for a *CP* violation signal in the Cabibbo suppressed decay $D^+ \to \pi^-\pi^+\pi^+$, using the 1 fb^{-1} of data collected 2011[19]. The $D^+ \to \pi^-\pi^+\pi^+$ and $D_s^+ \to \pi^-\pi^+\pi^+$ signals and the corresponding Dalitz plots are shown in Fig. 12. There are approximately 2.68 and 2.70 $\times$ 10^6 D^+ and D_s^+ decays, respectively.

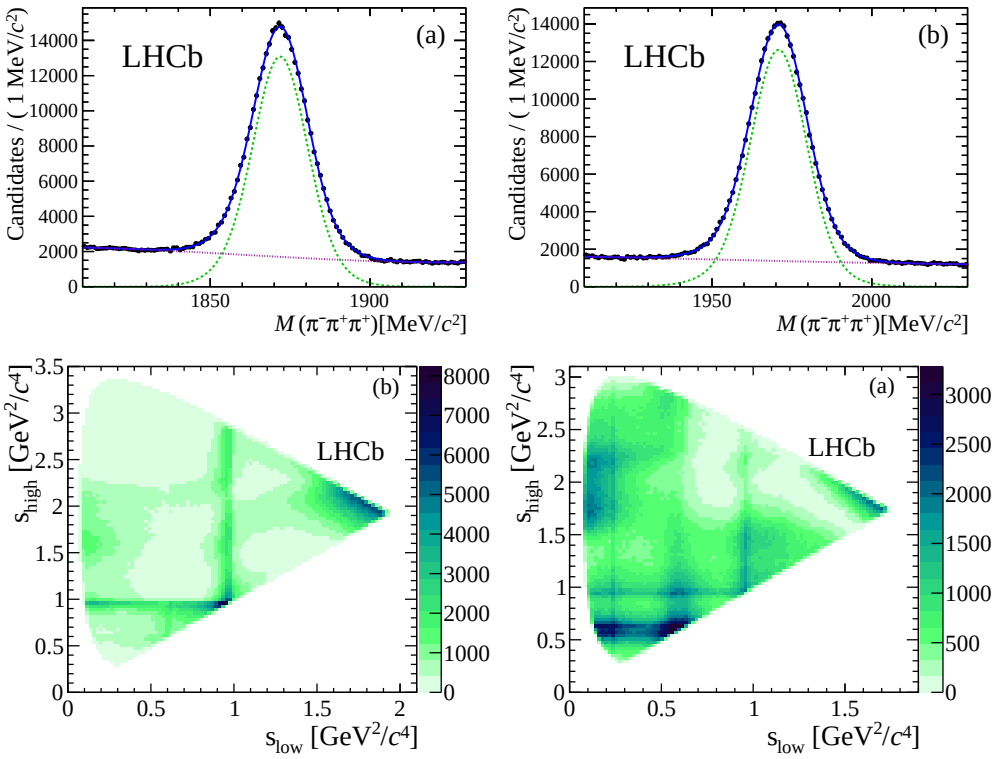

Figure 12: The $D^+, D_s^+ \to \pi^-\pi^+\pi^+$ signals and the corresponding Dalitz plots.

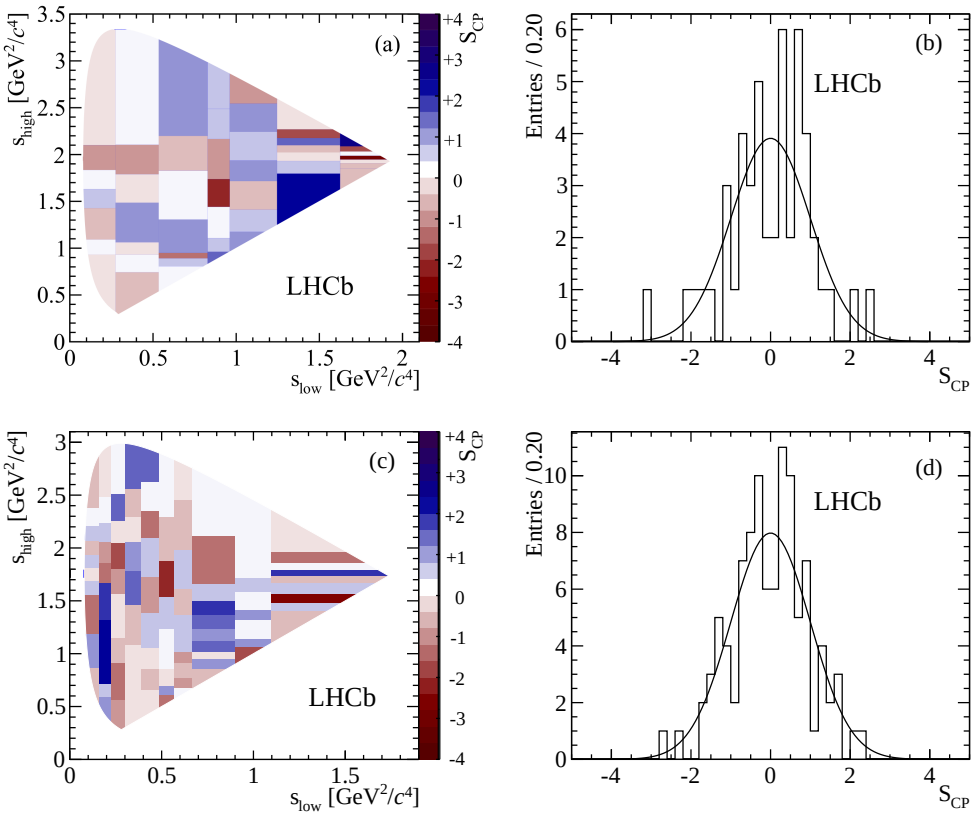

Figure 13: The distribution of S^i_{CP} across the $D^+ \to \pi^-\pi^+\pi^+$ Dalitz plot and the corresponding one-dimensional distributions.

The absence of localized asymmetries arising from instrumental and/or production effects are tested with the CF decay $D_s^+ \to \pi^-\pi^+\pi^+$. Inspection on the signal sidebands show that the background is also insensitive to any possible instrumental asymmetries. The anisotropy method is applied to $\pi^-\pi^+\pi^+$ candidates with invariant mass within a two σ interval around the D^+ mass.

Different bin divisions are tested. An adaptive scheme defines bins with equal population. As a cross-check, bins with equal size are also used. In each scheme tests are performed using different number of bins. The distribution of S^i_{CP} is shown in Fig. 13, together with the distribution across the $D^+ \to \pi^-\pi^+\pi^+$, for two examples of adaptive binning. No indication of *CP* violation was found.

3.4 Summary

Global fits to the existing measurements were performed HFAG collaboration [4], extracting the mixing and *CP* -violating parameters. The most general fit allows for

all types of *CP* violation. In the SM, however, direct *CP* violation in DCS decays is not possible. When this condition is imposed, from the four mixing parameters — x, y, $|q/p|$ and ϕ — only three become independent. A relation between the four parameters was obtained independently by Chiuchini *et al.* [22] and Kagan and Sokoloff [21] (a slightly different formula was also obtained by Grossman *et al.* [23]),

$$\tan\phi = \frac{x}{y}\left[\frac{1-|q/p|^2}{1+|q/p|^2}\right] \tag{11}$$

HFAG fit uses the formula to compute the averages. The impact of imposing this constraint is amazing, setting stringent bounds on $|q/p|$ and ϕ. The uncertainty in the value of $|q/p|$ allowing only for SM *CP* violation becomes 1.4%, and only a tenth of a degree for ϕ. The result of the HFAG global fits are summarized in Table 3.

HFAG also fits for the underlying theory parameters,

$$x_{12} \equiv \frac{2|M_{12}|}{\Gamma_D}, \quad y_{12} \equiv \frac{|\Gamma_{12}|}{\Gamma_D}, \quad \phi_{12} \equiv \arg\left(\frac{M_{12}}{\Gamma_{12}}\right):$$

$$\begin{aligned} x_{12} &= (0.43 \pm 0.14)\%, \\ y_{12} &= (0.60 \pm 0.07)\%, \\ \phi_{12} &= (0.9 \pm 1.6)^\circ. \end{aligned}$$

Contour plots with confidence level intervals from the *CP* violation-allowed fit are shown in Fig. 14, in the (x, y) plane, and in Fig. 15, in the $\phi, |q/p|$ plane. On the left panels contour plots from April 2013 are shown, whereas the right panel has the contours from May 2014. Note the change in the scale in both axes.

From Fig. 14 one sees that y is better constrained than x. The sign of y is well established. It is unlikely that x is a negative quantity, but one should stress that its central value differs from zero by less than three standard deviations. A more precise value of x will be achieved when new measurements from LHCb become available.

An impressive improvement is observed in the confidence intervals of the *CP* violation quantities ϕ and $|q/p|$, shown in Fig. 15, which is mostly due to the LHCb results of the $D^0 \to K^\mp\pi^\pm$ decay.

Important measurements with the full data set from Run I are under way in LHCb: y_{CP}, ΔA_{CP} with pion tagged D^0, x, y from $D^0 \to K^0_S\pi^-\pi^+$ time-dependent Dalitz plot analysis, A_Γ. With data from Run II, starting in 2015, the study of mixing will enter a new era of precision measurements. A significant improvement on the sensitivity of *CP* violation searches is also expected. However, for a correct interpretation of the experimental results, advances in theory are necessary. In particular, the ability of computing the hadronic matrix elements is a crucial step, allowing for a precise estimation of the SM contribution to both mixing and *CP* violation.

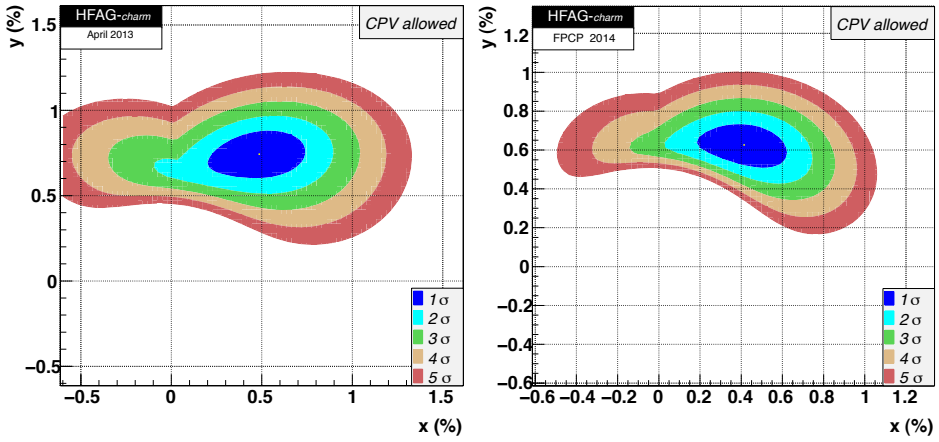

Figure 14: Contour plots in the x, y plane from a global fit to 41 measurements, allowing for CP violation. On the left we see the confidence intervals from the fit to the data available at April 2013. The plot on the right includes new measurements since April 2013. Reproduced from HFAG [4].

Table 3: Mixing and CP violation parameters obtained from a global fit of the existing measurements allowing for CP violation (from HFAG[4]).

parameter	CP violation allowed	no direct CP violation in DCS
$x(\%)$	$0.41^{+0.14}_{-0.15}$	$0.43^{+0.14}_{-0.15}$
$y(\%)$	$0.63^{+0.07}_{-0.08}$	$0.60^{+0.07}_{-0.08}$
$R_D(\%)$	$0.3489^{+0.0038}_{-0.0037}$	$0.3485^{+0.0038}_{-0.0037}$
$A_D(\%)$	$-0.71^{+0.92}_{-0.95}$	-
$\lvert q/p \rvert$	$0.93^{+0.08}_{-0.09}$	$1.007^{+0.014}_{-0.015}$
$\phi(^\circ)$	$-8.7^{9.1}_{-8.8}$	$-0.03^{0.10}_{-0.11}$

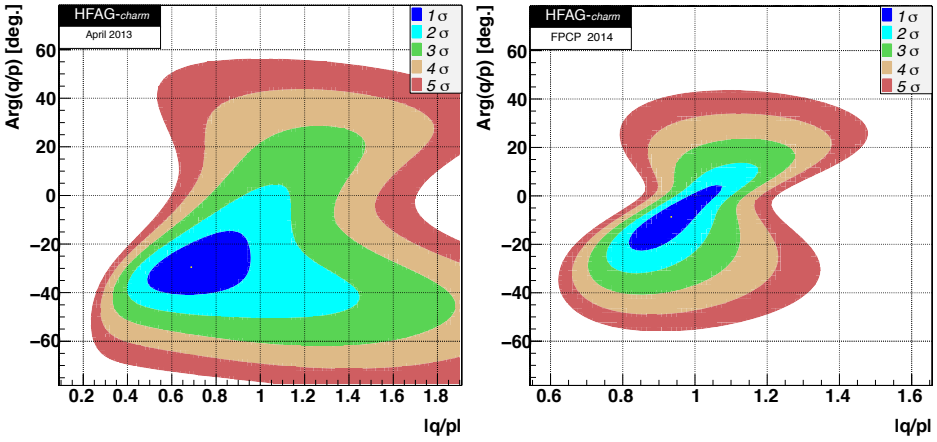

Figure 15: Contour plot of $|q/p|$ and its phase. On the left we see the confidence intervals from the fit to the data available at April 2013. The plot on the right includes new measurements since April 2013. Reproduced from HFAG [4].

ACKNOWLEDGEMENTS

I am grateful to the Brazilian Conselho Nacional de Desenvolvimento Científico e Tecnológico for partially supporting this work.

References

[1] Belle collab. (M. Staric *et al.*), *Phys. Rev. Lett.* **98** 091801 (2007).

[2] BaBar collab. (B. Aubert *et al.*) , *Phys. Rev. Lett.* **98**, 211802 (2007).

[3] CDF collab. (T. Aaltonen *et al.*), *Phys. Rev. Lett.* **100**, 121802 (2008)

[4] Heavy Flavor Averaging Group (Y. Amhis *et al.*), *arXiv:1207.1158* (online update at `http://www.slac.stanford.edu/xorg/hfag`; for the 2008 averages, see `http://www.slac.stanford.edu/xorg/hfag/charm/FPCP08/results_mix+cpv.html`).

[5] LHCb collab. (R. Aaij *et al.*), *Phys. Rev. Lett.* **111**, 251801 (2013).

[6] CLEO Collab. (D. Asner *et al.*), *Phys. Rev. D* **86**, 112001 (2012).

[7] BESIII Collab. (X-K. Zhou *et al.*), *arXiv:1403.1377* (2014).

[8] S. Bergmann, Z. Ligeti, Y. Nir and A. A. Petrov, *Phys. Lett.* **B 486**, 418 (2000).

[9] LHCb collab. (R. Aaij *et al.*), *Phys. Rev. Lett.* **112**, 041801 (2014).

[10] Belle Collab. (T. Peng *et al.*), *arXiv:1404.2412* (2014).

[11] BaBar Collab. (B. Aubert *et al.*), *Phys. Rev. Lett.* **100**, 061803 (2008).

[12] LHCb Collab. (R. Aaij *et al.*), *arXiv:1405.2797*.

[13] LHCb Collab. (R. Aaij *et al.*), LHCb-CONF-2013-003 (March 12, 2013).

[14] CDF Collab. (T. Aaltonen *et al.*), *Phys. Rev. D* **85**, 012009 (2012).

[15] B.R. Ko, Proceedings of the 36th International Conference on High Energy Physics (ICHEP2012), *arXiv:1212.1975* (2012).

[16] LHCb Collab. (R. Aaij *et al.*), in preparation.

[17] I. Bediaga *et al.*, *Phys. Rev. D* **80**, 096006 (2009).

[18] M. Willians, *Phys. Rev. D* **84**, 054015 (2011), *arXiv:1105.5338*.

[19] LHCb Collab. (R. Aaij *et al.*), *Phys. Lett. B* **728** 585 (2014).

[20] LHCb Collab. (R. Aaij *et al.*), *Phys. Lett. B***726**, 623 (2013).

[21] A. L. Kagan and M. D. Sokoloff, *Phys. Rev. D* **80**, 076008 (2009).

[22] M. Ciuchini *et al.*, *Phys. Lett.* **B** 655, 162 (2007).

[23] Y. Grossman, Y. Nir and G. Perez, *Phys. Rev. Lett.* **103**, 071602 (2009).